Colloids and Surfaces A: Physicochemical and Engineering Aspects 647 (2022) 129059

Contents lists available at ScienceDirect

Colloids and Surfaces A: Physicochemical and Engineering Aspects

journal homepage: www.elsevier.com/locate/colsurfa

Effect of nanoconfinement on the enzymatic activity of bioactive layer-by-layer assemblies in nanopores

Ievgen Kurylo, Sophie Demoustier-Champagne *, Christine Dupont-Gillain *

UCLouvain, Institute of Condensed Matter and Nanosciences - Bio and Soft Matter, Croix du Sud 1, box L7.04.02, 1348 Louvain-la-Neuve, Belgium

GRAPHICAL ABSTRACT

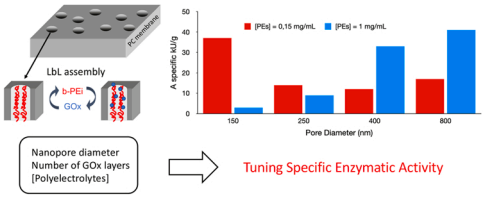

ARTICLE INFO

Keywords:
LbL assembly
Enzyme immobilization
Glucose oxidase
Nanopores
Nanobiocatalysis

ABSTRACT

In vivo, enzymatic reactions occur in confined environments. Such conditions can strongly improve enzyme behavior and are therefore interesting to study for further applications in biocatalysis. Here, we report on the influence of nanoconfinement on the catalytic properties of enzyme-based nanotubes, built by the layer-by-layer (LbL) assembly of branched polyethylenimine (bPEI) and glucose oxidase (GOx) in nanoporous polycarbonate membranes (PCm). More precisely, the influence of nanoconfinement on the biocatalytic activity is investigated by varying the number of (bPEI/GOx) bilayers, the concentration of polyelectrolytes (PEs) used for LbL deposition and the pore diameter of the PC membrane. Bicinchoninic acid (BCA) assay is employed to estimate the amount of enzyme loaded in the different LbL assemblies. The enzymatic activity was monitored, and found to depend on the three studied parameters. Typically, it decreases with decreasing pore diameter under high concentration of PEs, which may be attributed to limitations of substrate/product diffusion within the network formed in small pores. However, when lower concentration of PEs is used for the LbL assembly, the assemblies features a different macromolecular distribution and the enzymatic activity becomes optimal for low pore diameters. The results of this study pave the way to a more rational design of enzyme-loaded porous nanostructures for biocatalysis.

1. Introduction

Biocatalysis is a powerful and environmentally friendly approach based on application of enzymatic reactions [1]. The main advantages of using enzymes over inorganic catalysts are mild reaction conditions, higher efficiency, specificity and selectivity. In living organisms, control of complex networks of chemical reactions often occurs via surface- and volume-confined enzymes. These nanoconfinement effects are in core of improving the enzymatic activity and stability and they facilitate cascade reactions within cells [2]. The reason for this is that enzymatic activity is affected by conformational changes, availability of intact active site and substrate binding reaction rate [3]. All these interesting

* Corresponding authors.
E-mail addresses: sophie.demoustier@uclouvain.be (S. Demoustier-Champagne), christine.dupont@uclouvain.be (C. Dupont-Gillain).

https://doi.org/10.1016/j.colsurfa.2022.129059
Received 20 January 2022; Received in revised form 19 April 2022; Accepted 19 April 2022
Available online 22 April 2022

features serve as a driving force for developing synthetic structures, mimicking confined environments of enzymes in nature.

Among the different available strategies of enzyme encapsulation, such as micellar systems [4], microdroplets [5], DNA origami nanoreactors [6], and hollow capsules [7,8], enzymatic nanotubes present several major advantages. Apart from high surface to volume ratio, nanotubes offer the possibility to easily load the internal space with guest molecules [9]. Nanotubes can also stabilize enzymes by offering a protective shell and substantially facilitate recovery of enzymes after use. A particularly efficient and highly versatile strategy to prepare tubular nanomaterials with tailored properties consists in the template-assisted synthesis combined with layer-by-layer (LbL) assembly into the nanopores of a sacrificial membrane [10]. Alternate deposition of oppositely charged entities, such as proteins and polyelectrolytes (PEs) [11] into the nanopores of track-etched polycarbonate membranes, has successfully led to the formation of various bioactive multilayered micro- and nanotubes [9,12–18]. Some interesting and unique features of the LbL assembly technology are its ability to allow protein encapsulation in mild aqueous conditions and the possibility to build-up multilayered films with tunable thickness as well as tunable internal and surface compositions and structures. Owing to these advantages, immobilization of enzymes using the LbL assembly method has found a variety of biomedical applications [19], such as drug delivery systems [20], antibacterial coatings for implants [21] or biosensors [22] but also, in the energy domain as high power enzymatic biofuel cells [23,24].

The effect of nanoconfinement on the LbL growth mechanism has been investigated by our group, using a well-known synthetic polyelectrolyte system, the poly(allylamine hydrochloride)/poly(sodium 4-styrenesulfonate) (PAH/PSS) pair [25]. This study showed that the LbL assembly mechanism inside nanopores is significantly different from that on planar open surfaces and presents two different regimes related to the growth kinetic. In the first regime, a growth mechanism similar to the one on planar surfaces was observed. As the internal pore size decreases with the build-up of LbL multilayers, the LbL growth enters into the second regime, which is kinetically much slower due to the formation of a dense gel inside the pores. The main factors determining the transition point between the two regimes were found to be the pore diameter and the multilayer thickness. Cho and coworkers also investigated the effect of pore size on the formation of LbL tubular structures. Their study led to similar conclusions: LbL assembly in nanochannels is strongly governed by the geometrical characteristics of the template and exhibits a strong dependence on PEs assembly conditions (e.g. pH and ionic strength) [26].

The impact of assembly conditions on the activity of LbL-assembled enzymatic nanotubes was reported in a few papers. Caruso and coworkers investigated the preparation of LbL enzyme/PE multilayers on polycarbonate membranes with two different pore diameters (400 and 100 nm) [13]. In this study, they showed that the bioactivity was related to the total surface area of the membrane, which is governed by the pore size and density, and the number of deposited enzyme layers. They, however, did not quantify the amount of enzyme incorporated into the nanotubes. In a preceding paper, we reported on the comparison of thin films including a different number of enzyme layers built on flat silicon wafers and within 200 nm cylindrical pores of polycarbonate membranes [27]. In each case, the amount of enzyme loaded in the different LbL films was determined and correlated with enzyme activity. Film growth and enzyme loading were shown to occur faster in the confined medium, and the enzyme weight fraction was high and remained constant along the build-up in the nanopores. Conversely, the relative amount of enzyme in flat films significantly decreased with the number of layers due to partial exchange with PEs upon growth. This study also emphasized that enzyme immobilization through LbL assembly in confined media can lead to very active surfaces with a restricted number of LbL cycles. In a more recent study, Komatsu and coworkers showed that the catalytic activity of glucose oxidase (GOx)-based LbL microtubes ($\pm$ 1 μm outer diameter) depends on the GOx layer position in the cylindrical wall [18]. Some other works, where the enzyme was immobilized by another method than LbL assembly into nanochannels, also demonstrated the impact and importance of spatial confinement on GOx activity and reaction kinetics [28,29]. Even though these studies highlight some interesting features of enzyme confinement in nanochannels, further investigations are still needed to gain a better and deeper understanding of the influence of nanoconfinement effects on enzymatic activity in synthetic nanostructures. Indeed, to our knowledge, up to now, no study jointly combined the evaluation of the impact of the LbL assembly conditions and enzyme confinement on film growth, enzyme loading, and biocatalytic efficiency.

In the present study, we therefore investigate in details the influence of surface and volume nanoconfinement effects on enzymatic activity in LbL-assembled embedded nanotubes. By surface and volume confinement, we mean enzymatic reactions carried out on a solid support and within micro/nano-compartments, respectively. For that purpose, branched polyethyleneimine (bPEI)/glucose oxidase (GOx) multilayer films were prepared by LbL assembly within nanoporous polycarbonate membranes (PCm) presenting various pore diameters. Nanotubes still embedded within the templates were investigated as they only feature an inner surface, what differentiates them from flat films and allows to better address the nanoconfinement effect. Glucose oxidase (GOx) was selected as model enzyme for this work as it is a robust and well-studied enzyme with known 3D structure. Moreover, GOx has a considerable importance for many applications and in particular in glucose biosensors. Branched polyethylenimine (bPEI) was used as a counter-charged polyelectrolyte as its ability to be readily LbL-assembled with GOx without substantial desorption of the enzyme has been demonstrated [30], which could be a strong issue when other polycations (e.g. PDMA, PAH) are used [31]. Moreover, in a preceding work, we optimized the conditions for the elaboration of stable bPEI/GOx nanotubes by the template-assisted method [14]. The surface confinement effect is addressed by comparing the enzymatic loading and activity of embedded nanotubes assembled using different concentrations of PEs in the LbL build-up solution, while the volume confinement effect is assessed by performing the LbL assembly within PCm of different pore diameters.

2. Materials and methods

2.1. Materials

bPEI (average Mw ~25,000 by LS) and GOx (from *Aspergillus niger*, Type X-S, lyophilized powder, 145,200 units/gram, isoelectric point is 4.2) were purchased from Sigma-Aldrich and used as positive and negative polyelectrolytes, respectively. MES (2-(4-morpholino)ethanesulfonic acid, monohydrate, Acros Organics) buffer solution (10 mM, pH 6.5) was used as the medium for assembly. Polyelectrolyte solutions were prepared with a concentration of either 0.15 or 1 mg mL^{-1}. Track-etched polycarbonate membranes (PCm) with nominal 150, 250, 400 and 800 nm pore diameters, 25 μm thickness (24 μm for 800 nm PCm) and a pore density of $4{\cdot}10^7$ cm^{-2}, were provided by it_4ip company, Louvain-la-Neuve, Belgium (http://www.it4ip.be/). The characteristics of the PCm used in this study are gathered in Table S1. GOx assay kit (based on the study of coupled reaction of oxidation of glucose, followed by oxidation of p-hydroxybenzoic acid and 4-aminoantipyrine via released H_2O_2) was purchased from Megazyme. BCA protein assay was purchased from Thermo Scientific.

2.2. LbL assembly of bPEI/GOx into nanopores

The enzyme-containing nanotubes embedded in polycarbonate membranes were fabricated according to the procedure shown in Fig. 1. PE multilayers were deposited by alternately dipping the PCm support in bPEI and GOx solutions. Two conditions were tested: concentrations of

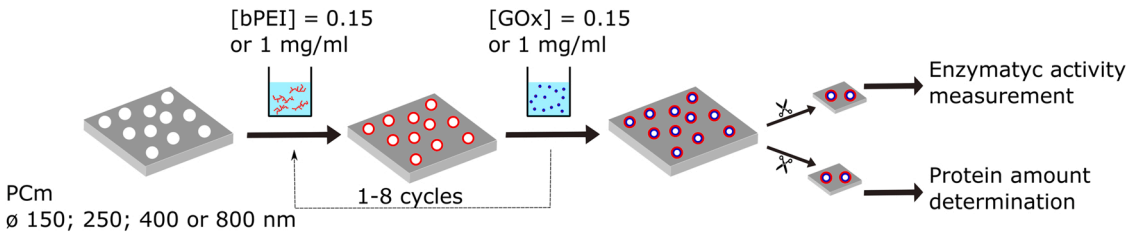

Fig. 1. Schematic representation of the fabrication of enzyme nanotubes embedded in PC membrane with indication of the different experimental parameters that were varied and the type of characterization that were performed in the present study.

both PEs were either 0.15 mg mL^{-1} or 1 mg mL^{-1}. The build-up started with bPEI adsorption, followed by two rinsing steps in MES buffer (2 min each) to remove loosely attached PE chains. Then, the surface with an excess of positive charge was dipped in GOx solution and rinsed twice to complete one LbL cycle. Ultrasonication was applied during 15 min to facilitate the diffusion of PEs into the pores. The total adsorption time was 40 min for one PE layer deposition. After every cycle, a cell scraper was used to scrub out the film that grew on the two external surfaces of the membrane, as it would block pore entry. This process was repeated until the desired number of cycles (from 1 to 8) was achieved. A piece (~1.5 cm^2) of every sample was cut, immersed in DI water for 30 s to remove the remaining salt from buffer solution, air-dried and stored at 4 °C. The complete procedure is illustrated on Fig. 1.

2.3. Enzymatic activity assay

GOx activity was measured by colorimetric assay based on oxidation of p-hydroxybenzoic acid and 4-aminoantipyrine by the generated H_2O_2 in presence of peroxidase (POD) (see Equation (2)), where H_2O_2 is the product of glucose oxidation by oxygen, catalyzed by GOx (see Equation (1)).

.

A round piece of sample (1 mm diameter) was cut with a puncher and dipped in 50 µL of MES buffer in 96-well microplate. After that, 200 µL of POD mixture (containing peroxidase, p-hydroxybenzoic acid, 4-aminoantipyrine and stabilizers, final pH 7.0) and 50 µL of 90 mg mL^{-1} D-glucose (this concentration was recommended by the assay kit provider, based on concentrations of the POD mix components) were added in each well. Reaction was initially inhibited by cooling down with a cold pack in order to compensate deviations from different addition time of the reagents. Then light absorbance at 510 nm (A_{510}) was recorded for 30 min in a kinetic mode under continuous shaking. Each sample was analyzed in triplicate. Activity was determined using a calibration curve, made simultaneously with the samples. Maximal number of samples per analysis was kept at 30 (for a given pore size: 3 samples for every number of bPEI/GOx bilayers (1−8) + 6 calibration standards).

2.4. BCA assay

A 2 × 2 or 5 × 5 mm^2 square piece was cut from samples prepared with 1 or 0.15 mg mL^{-1} of PEs respectively, and was immersed in 400 µL of mixture of BCA test reagents A and B (50:1) in a 3 mL glass tube, tightly closed and incubated during 2 h at 70 °C in a water bath. After that, solution was cooled down to room temperature and the condensate on the top of the tube was carefully mixed with solution on the bottom. Then 200 µL of this solution was poured in 96-well plate and light absorbance was measured at 562 nm (A_{562}). The same sample was submitted a second time to the same procedure in order to maximize protein recovery. The enzyme amount was determined using a calibration curve, made from free GOx solutions of known concentration analyzed in the same conditions.

An independent experiment was performed in order to estimate the accuracy and reproducibility of the BCA assay. For that purpose, a sample of $(PEI/GOx)_6$ embedded nanotubes with 800 nm pore size was prepared. 5 pieces of this sample (3 ×3 mm^2 size) were analyzed with the BCA assay in parallel using the usual protocol. Standard deviations of the measurements and completeness of extraction upon each step were estimated. The data are presented in Table S2. The total extracted amount was found to be 23.9 (± 3.7) µg.cm^2, and 86% of this amount was recovered after the first extraction step.

2.5. Scanning Electron Microscopy (SEM)

The morphology of nanotubes was investigated with a field emission scanning electron microscope (JSM-7600F, JEOL Ltd.), operated at 15 kV. Samples were prepared by the following procedure: $(bPEI/GOx)_n$ nanotubes were freed from the template by dissolving the PCm in CH_2Cl_2, then the nanotube suspension was filtered through 100 nm PET membranes covered by 20 nm of gold (Cressington Sputter Coater 208HR), and further rinsed several times with pure CH_2Cl_2 prior to SEM observation.

3. Results and discussion

3.1. Construction of enzyme-containing multilayers within nanopores

In order to explore the impact of nanopore size on bioactivity, bPEI/GOx nanotubes were grown by LbL assembly in PC membranes with various well-defined pore diameters ranging from 150 to 800 nm, according to the procedure described in Fig. 1. Nanotubes were fabricated under the previously reported optimized assembly conditions[14], i.e. LbL assembly from 10 mM MES buffer solutions at pH 6.5. In the present work, polyelectrolyte concentrations in the deposition solution were however varied in order to obtain embedded nanotubes presenting different multilayer morphology. Moreover, to establish a correlation between enzyme activity and both enzyme loading and stratified nanotube wall structure, samples containing from 1 to 8 enzyme layers were prepared for each pore size.

First, to check if the LbL assembly of PEI/GOx within PCm nanopores

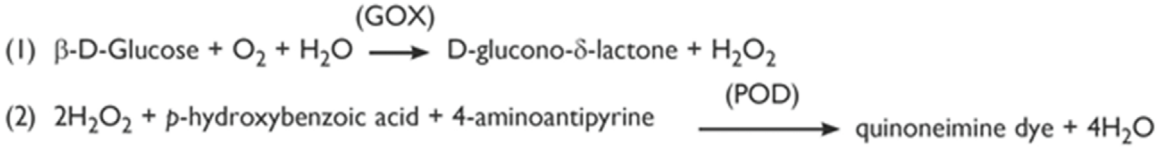

was successful under the chosen conditions, some samples were de-templated by dissolution of the PCm in dichloromethane (Fig. 2(a)) and the collected nano-objects were characterized by SEM. As shown on Fig. 2(c), for a representative system built within nanopores of 400 nm and using [PEs] = 1 mg mL^{-1}, free intact (bPEI/GOx)$_6$ nanotubes, replicating the PCm nanopores, are observed after the dissolution of the template. The length of most of the tubes corresponds to the membrane thickness (25 μm), confirming that enzyme-based multilayers are uniformly formed on the entire length of the nanopores. On Fig. 2(b), we present a SEM picture of the surface of the membrane containing the embedded LbL (bPEI/GOx)$_6$ nanotubes prior to the dissolution of the membrane.

3.2. Enzyme activity of the multilayer assemblies in nanopores

For each pore size, two series of samples were prepared using a low and a high initial concentration of PEs for the LbL assembly. The enzymatic activity of all samples was then measured by colorimetric assay. The obtained data are presented in different ways in Fig. 3. First, the evolution of the enzymatic activity of LbL-assembled GOx-based nanotubes, embedded in PCm of different pore diameters and built-up under either 0.15 mg mL^{-1} or 1.0 mg mL^{-1} initial concentrations of PEs, related to the total area of the sample, S_{sample} (i.e. the surface area of the piece of membrane used for measurement) in terms of the number of bPEI/GOx bilayers, is presented in Fig. 3(a,b).

In order to take into account the difference in active surface area between the different samples, the enzymatic activity was also normalized to the calculated (see Table S1) internal surface area of the pores (Fig. 3. c,d). Finally, to study how enzymatic activity is evolving with increasing number of enzyme layers for a given pore diameter, the enzymatic activity normalized to the activity for the first bilayer is presented in Fig. 3(e,f).

When the enzymatic activity is simply related to the surface area of the membrane sample, two main trends in the evolution of the enzymatic activity are observed (Fig. 3a,b). First, under both investigated assembly conditions, the bioactivity is increasing with PCm pore diameter. Secondly, as expected, the bioactivity is higher for all the samples prepared under the highest tested concentration of PEs (1.0 mg mL^{-1}), and this is more marked as the pore diameter increases.

When the enzymatic activity is related to the total internal surface of the pores (S_{pores}), meaning that the difference in internal surface area of the pores between the different sample is taken into account, a clear impact of the confinement (pore diameter) is appearing (Fig. 3c,d). For the low concentration of PEs (0.15 mg mL^{-1}), the bioactivity is increasing almost linearly with the number of (bPEI/GOx) bilayers for all pore sizes and, no significant impact of the pore diameter on bioactivity is detected. In contrast, for the samples prepared under higher concentration of PEs (1.0 mg mL^{-1}), a clear influence of the pore diameter on the enzymatic activity is observed and this impact is stronger with increasing number of bilayers.

Specifically, the activity, related to the internal surface of the pores, for the first bilayer is nearly identical for all the investigated pore sizes. For two and higher number of bilayers, a progressive but clear difference in bioactivity is observed in terms of pore diameters. When looking to the values of A/S_{pores} for a fixed pore diameter, we observed that the bioactivity increases until a certain number of bilayers is reached and further decreases to finally reach a plateau for the 150 and 250 nm pore size samples. The observation of a maximum in the bioactivity of embedded nanotubes is attributed to the interplay between the amount of enzyme embedded in the tubes and the accessibility of glucose to the enzyme, as reported previously by our group.[14] Moreover, the data reported in Fig. 3d shows that this maximum of bioactivity depends on pore size, appearing after 2 bilayers for the small pore diameters (150 nm and 250 nm) and only around 5–6 bilayers for the larger pores (400 and 800 nm).

Finally, looking at the evolution of the enzymatic activity normalized to the activity for the first bilayer (A_n/A_1) in terms of the number of bilayers allows to reveal the impact of the structure of the multilayer on the bioactivity. When built-up under the higher investigated [PEs] (1 mg mL^{-1}), except for the smaller pore sizes (150 nm), a strong

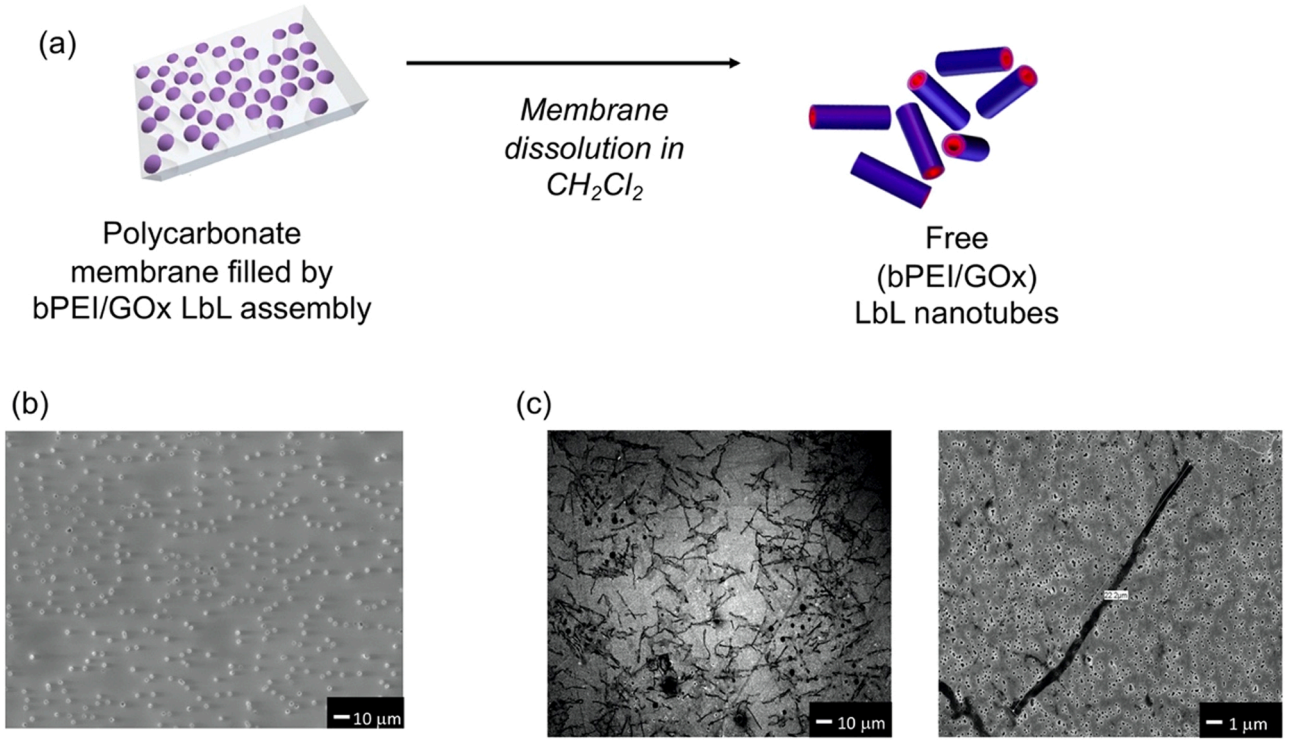

Fig. 2. (a) Scheme illustrating the procedure followed to release nanotubes from the membrane prior to SEM observations; (b) SEM picture of (bPEI/GOx)$_6$ nanotubes still embedded into the PC membrane; (c) free (bPEI/GOx)$_6$ nanotubes observed by SEM after PC membrane dissolution in dichloromethane.

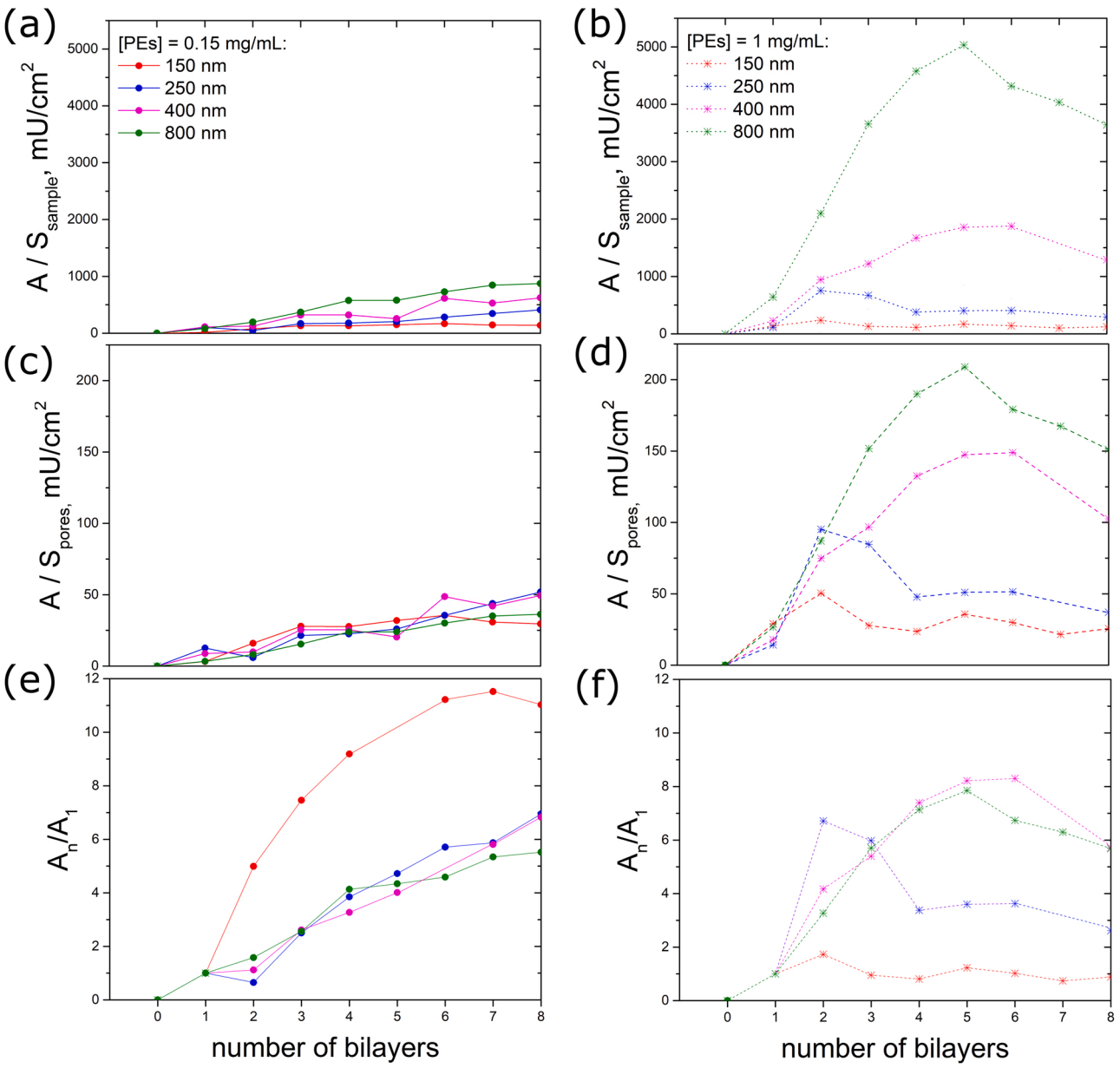

Fig. 3. Enzymatic activity of LbL-assembled GOx-based nanotubes embedded in PCm of different pore diameters and built-up under two different initial concentrations of PEs: 0.15 mg mL^{-1} (a,c,e) and 1.0 mg mL^{-1} (b,d,f) in terms of the number of bilayers, related to: total area of the sample, S_{sample} (a,b), total internal surface of the pores, S_{pores} (c,d), activity value for the first bilayer A_1 (e,f). The dotted and solid lines are drawn to guide the eye.

increase of the enzymatic activity is observed after the first bilayer deposition (Fig. 3f). These data might be explained by changes occurring in the LbL build-up process after the assembly of the first bilayer that may lead to a rearrangement of enzyme layers in which GOx adopt a more favorable conformation leading to a higher activity, as suggested by Xie et al. [32]. When built-up under the lowest investigated [PEs] (0.15 mg mL^{-1}), the relative enzymatic activity (A_n/A_1) is increasing in a very similar and linear way with the number of bilayers way for all samples, except again for the (bPEI/GOx) assembled in 150 nm pore size which presents a much more rapid increase of the enzymatic activity (Fig. 3e). These data already demonstrate that confining enzymes in small nanochannels can strongly impact their activity.

3.3. Enzyme content in multilayer assemblies

In order to determine the specific enzymatic activity, we performed BCA tests on several series of samples to quantify the protein amount in the different nanotubes. The evolution of the protein mass (m) related to the total internal surface of the pores (S_{pores}) as a function of the number of deposited (b-PEI/GOx) bilayers for different membrane pore sizes and initial concentrations of PEs used for the LbL assembly is presented on Fig. 4. These results show that for all pore sizes, $m_{protein}/S_{pores}$ is higher when the enzyme-based multilayers were built-up under the highest tested [PEs]. The amount of immobilized protein in nanotubes is generally increasing during the built-up of the 2–4 first deposited bilayers (depending on the pore size) and further, remains almost constant. The rate of this increase of protein amount is also generally greater for the samples prepared with [PEs] = 1 mg mL^{-1}. The protein mass variation per surface area of the pores features a relationship with pore diameter: with the smallest pore diameter, it does not increase much with the number of deposited bilayers, while it globally tends to increase with the number of bilayers in larger pores, even though saturation may be reached after a few bilayers deposition at the highest concentration.

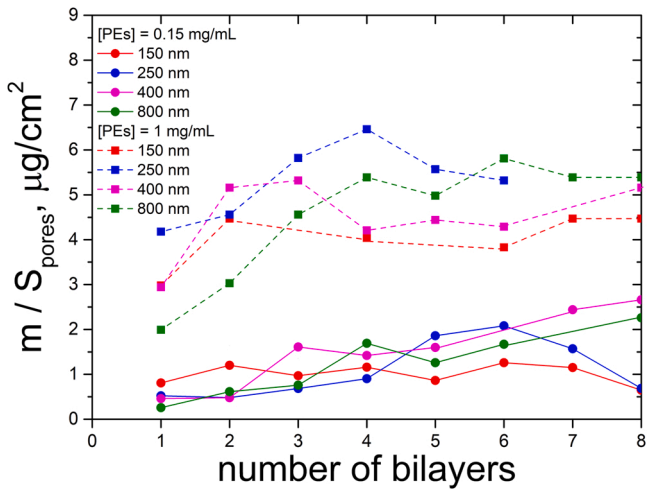

Fig. 4. Amount of GOx (m) immobilized in PCm related to the total internal surface of the pores (S_{pores}) as a function of the number of deposited (bPEI/GOx) bilayers for different membrane pore sizes and initial concentrations of PEs used for the LbL assembly.

3.4. Correlation between enzyme activity, enzyme content and multilayer structure

To investigate more deeply the impact of the nano-environment on enzyme bioactivity, the specific enzymatic activity of GOx-based nanotubes embedded in PCm of different pore diameters (150, 250, 400 and 800 nm) and built under two different initial concentrations of PEs (0.15 and 1.0 mg mL^{-1}) is presented in Fig. 5 as a function of the number of (b-PEI/GOx) bilayers.

First, these data show that the specific activity can be finely tuned by playing on the different investigated parameters: size of the pores, polyelectrolyte concentration used for the multilayer assembly and number of layers. Secondly, an important general trend is clearly observed: for multilayers built-up in small pores (Φ_{pores} = 150 and 250 nm), the highest specific GOx activity is obtained when the assembly is performed under low [PEs] (0.15 mg mL^{-1}), while for multilayers built-up in larger pores (Φ_{pores} = 400 and 800 nm), the highest specific activity is obtained when the assembly is made under high [PEs] (1 mg mL^{-1}).

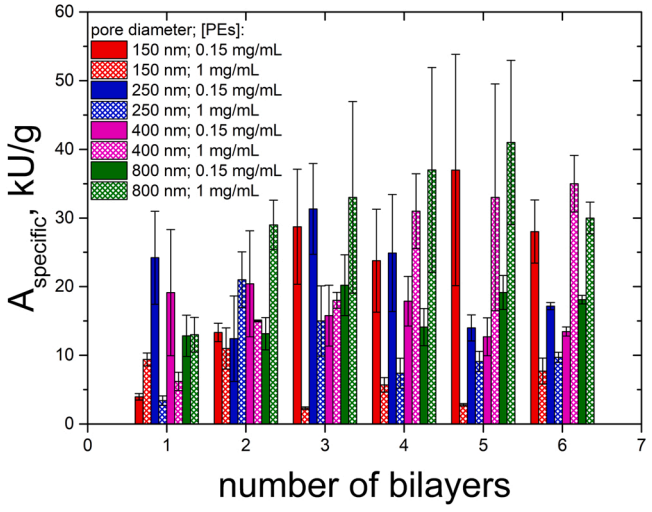

Fig. 5. Specific enzymatic activity of GOx-based nanotubes embedded in PCm of different pore diameters (150, 250, 400 and 800 nm) and built-up under two different initial concentrations of PEs (0.15 and 1.0 mg mL^{-1}) as a function of the number of (bPEI/GOx) bilayers.

To better highlight this observation, the evolution of the specific enzymatic activity for the five bilayer samples ($(bPEI/GOX)_5$) nanotubes grown under two different concentrations of PEs is presented in Fig. 6 as a function of PCm pore diameters.

Within large pores (Φ = 400 and 800 nm), the specific enzymatic activity is significantly lower when the bPEI/GOx nanotubes are built under low concentration of PEs (0.15 mg mL^{-1}), while the opposite trend is observed for smaller pores (Φ = 150 nm and 250 nm) where a higher specific enzymatic activity is obtained for bPEI/GOx nanotubes built under low [PEs]. Moreover, the specific enzymatic activity for the 150 nm pore size samples built up under low [PEs] is almost equivalent to the specific activity reached for the 800 nm pore size samples built up under high [PEs]. This confinement effect is very interesting from an application point of view, as it reveals that high specific activity can also be reached using low amount of enzyme to prepare the sample.

Our data on protein amount in pores with different diameters depending on the number of deposited layers and on PE concentration (see Fig. 4) suggest that the distribution of enzyme (GOx) and counter polyelectrolyte (bPEI) in the pores may be depicted as illustrated by Fig. 7. Such interpretation is based on the profile of layers growth as investigated in our previous study [25], but remains however partly speculative since the amount of deposited counter polyelectrolyte, in contrast with the one of enzyme, was not monitored. When pore diameter is smaller, a network is formed earlier, after a few deposition steps only, while in larger pores, deposition would mainly occur on the pore walls, leaving an open lumen in the core of the pores (Fig. 7a). In the latter case, it is only after the deposition of a higher number of bilayers that a network would finally form (Fig. 7b). Finally, when deposition occurs from solutions at low concentration, the protein load is lower. As there is, however, no strong increase of protein content with the number of deposition steps within small pore diameters, there is possibly also the formation of a network that decreases the ability to deposit more material upon successive steps of deposition. This network would then be less dense or would contain a higher counter-polyelectrolyte amount if compared to the one formed at a higher concentration (Fig. 7c).

The variations of specific activity as a function of PE concentration used for build-up and of pore diameter may then be discussed in light of these different architectures of these assemblies of enzyme and counter-polyelectrolyte deposited inside the pores. The major impact on enzymatic activity of different pore diameters in case of multilayers built with [PEs] = 1 mg mL^{-1} could be attributed to substrate/product diffusion restrictions, as an increase of specific activity is observed with

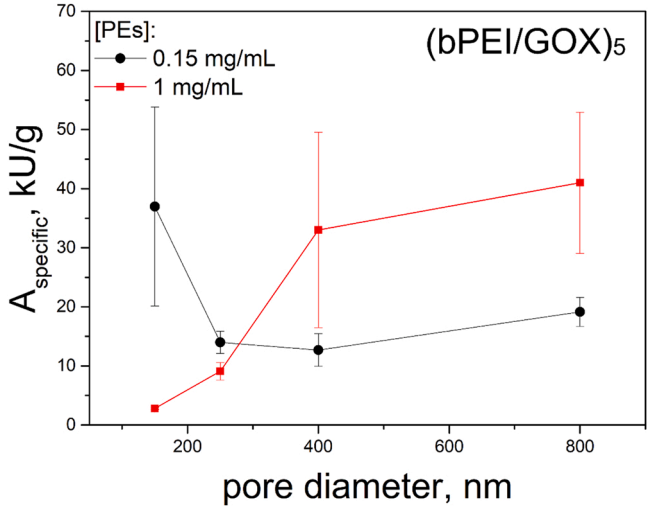

Fig. 6. Specific enzymatic activity of $(bPEI/GOX)_5$ nanotubes grown under two different concentrations of PEs as a function of PCm pore diameters. Error bars show the standard deviation.

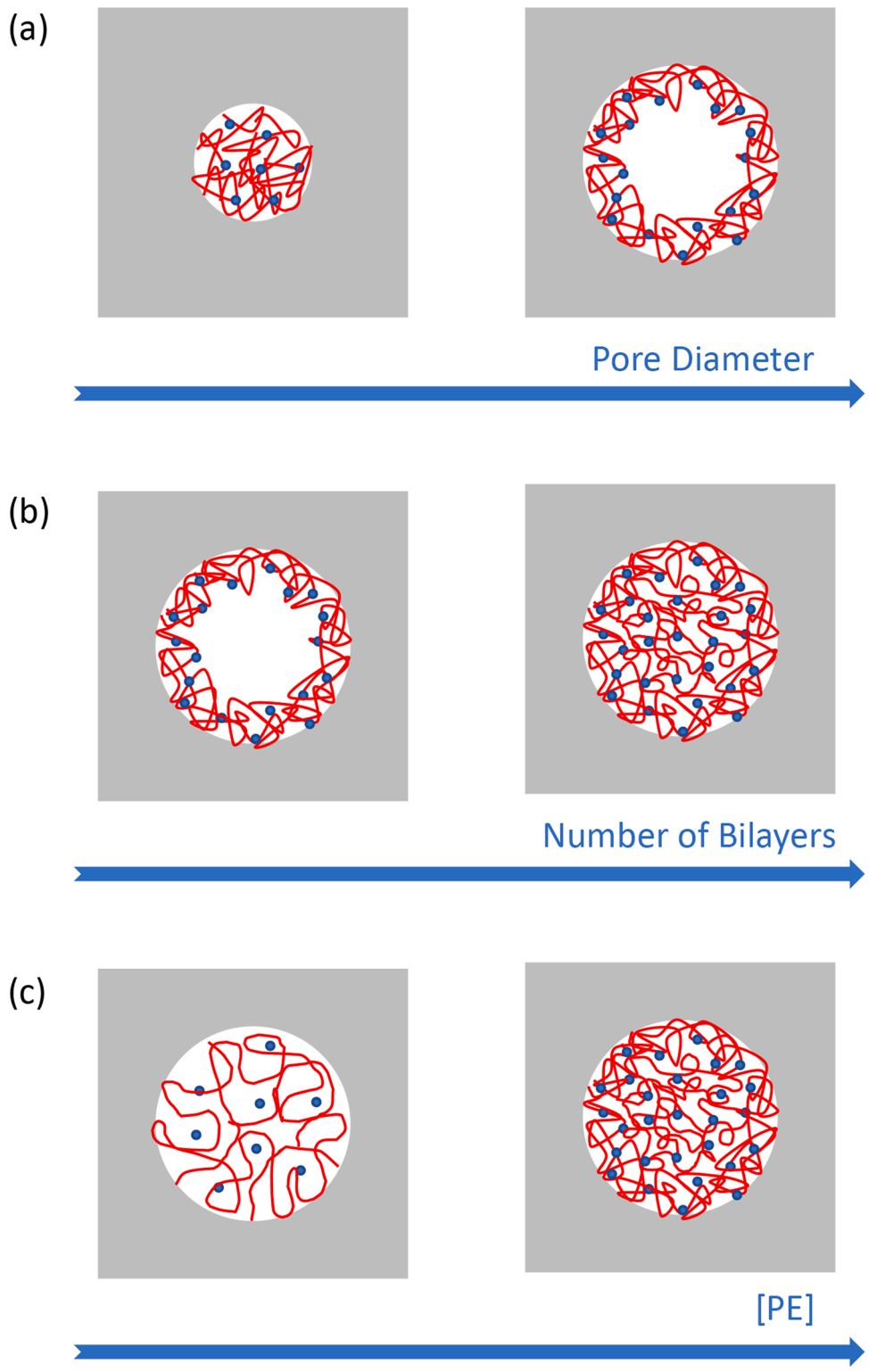

Fig. 7. Schematic representation of the LbL assembly build-up in small and large pores (a), for increasing number of bilayers (b) and for low and high PEs concentration (c).

pore diameter. These layers feature a higher protein content than the ones obtained at low [PEs], so the availability of the whole protein load to the substrate is restricted. It is, however, improved when exchanges between the immobilized phase and the solution are increased with the larger pore diameters owing to the central lumen that may stay open in the heart of the pores when the diameter is large enough, while the formation of a network of macromolecules limits the exchanges to slow diffusion processes for small pore diameters. On the other hand, the higher specific activity observed with smaller pore diameters (150 and 250 nm) in case of [PEs] $= 0.15$ mg mL^{-1} indicates a favorable confinement effect. At this concentration, the protein load is lower. According to the better specific activity in pores with small diameter, diffusion limitations may become less important, and the layer architecture, i.e. the respective distribution of enzyme vs counter

polyelectrolyte molecules, may then play a more important role. A higher amount of counter polyelectrolyte in the system may provide a more hydrated environment thereby keeping a higher enzymatic activity, while in larger pores, if a lumen is kept, the protein molecules may remain closer to the pore walls in a less active conformation or less available to the substrate. Another possible explanation would be that the network that is formed when a low PE concentration is used is less dense, and would thus be more favorable to substrate and product diffusion.

To sum up, the balance between a more favorable architecture for diffusion vs for enzyme activity is better in large pores when layers are built from a high concentration solution, while it turns out to be better in pores with smaller diameters when solutions at low concentrations are used. The confinement effect observed in small pores filled from solutions at low concentration may be helpful to keep a high specific activity, a much wanted feature especially when only limited amounts of enzyme are available or when their production is very expensive.

4. Conclusion

(bPEI/GOx) multilayers embedded nanotubes were successfully synthesized via LbL method in combination with template synthesis in PC membranes. Their formation was confirmed by SEM imaging of liberated nanotubes. Different LbL growth regimes were achieved by varying the PE concentration and pore diameters of the PC templates. A nanoconfinement effect on the enzymatic activity was revealed for nanotubes prepared with low concentrations of PE, whose specific enzymatic activity was higher for smaller pore diameters. On the other hand, when a higher PE concentration was used, the specific enzymatic activity was higher for larger pore diameters. Based on the enzyme amount as a function of the number of deposited layers and of the concentration used to build the layers, these variations of the specific enzymatic activity may be explained by the more or less favorable substrate/product diffusion within the pores as well as by the different distribution of Gox and bPEI. While smaller pores are more readily filled with a macromolecular network that limits diffusion, they may promote the formation of a less dense or more hydrated system, resulting in a higher enzymatic activity. Our study allows the mechanisms underlying enzymatic activity in confined spaces to be better understood. A rationale is thus developed to select optimal parameters for enzyme deposition into porous systems, which can be strongly beneficial for further developments of nano-biocatalysts.

CRediT authorship contribution statement

Ievgen Kurylo: Methodology, Investigation, Writing – original draft. **Sophie Demoustier-Champagne:** Conceptualization, Supervision, Writing – original, draft, Writing – review & editing. **Christine Dupont-Gillain:** Conceptualization, Supervision, Writing – original draft, Writing – review & editing.

Declaration of Competing Interest

The authors declare no competing interests.

Acknowledgements

This work was supported by the F.R.S.-FNRS for its financial support (T.0080.19 - PDR project). The authors thanks Etienne Ferain form It4ip for providing the PC membranes.

Appendix A. Supporting information

Supplementary data associated with this article can be found in the online version at doi:10.1016/j.colsurfa.2022.129059.

References

[1] R. Wohlgemuth, Biocatalysis – key enabling tools from biocatalytic one-step and multi-step reactions to biocatalytic total synthesis, New Biotechnol. 60 (2021) 113–123, https://doi.org/10.1016/j.nbt.2020.08.006.
[2] A. Küchler, M. Yoshimoto, S. Luginbühl, F. Mavelli, P. Walde, Enzymatic reactions in confined environments, Nat. Nanotechnol. 11 (2016) 409–420, https://doi.org/10.1038/nnano.2016.54.
[3] Z.D. Nagel, J.P. Klinman, A 21st century revisionist's view at a turning point in enzymology, Nat. Chem. Biol. 5 (2009) 543–550, https://doi.org/10.1038/nchembio.204.
[4] T.E. Sintra, S.P.M. Ventura, J.A.P. Coutinho, Superactivity induced by micellar systems as the key for boosting the yield of enzymatic reactions, J. Mol. Catal. B Enzym. 107 (2014) 140–151, https://doi.org/10.1016/j.molcatb.2014.06.001.
[5] Y. Liu, S.Y. Jung, C.P. Collier, Shear-driven redistribution of surfactant affects enzyme activity in well-mixed femtoliter droplets, Anal. Chem. 81 (2009) 4922–4928, https://doi.org/10.1021/ac900624h.
[6] V. Linko, M. Eerikäinen, M.A. Kostiainen, A modular DNA origami-based enzyme cascade nanoreactor, Chem. Commun. 51 (2015) 5351–5354, https://doi.org/10.1039/C4CC08472A.
[7] A.S. Pereira, C.P.L. Souza, L. Moraes, G.C. Fontes-Sant'Ana, P.F.F. Amaral, Polymers as encapsulating agents and delivery vehicles of enzymes, Polymers 13 (2021) 4061, https://doi.org/10.3390/polym13234061.
[8] F. Cuomo, A. Ceglie, A. De Leonardis, F. Lopez, Polymer capsules for enzymatic catalysis in confined environments, Catalysis 9 (2019) 1, https://doi.org/10.3390/catal9010001.
[9] T. Komatsu, Protein-based nanotubes for biomedical applications, Nanoscale 4 (2012) 1910–1918, https://doi.org/10.1039/C1NR11224D.
[10] S. Zhang, F. Xia, S. Demoustier-Champagne, A.M. Jonas, Layer-by-Layer assembly in nanochannels: assembly mechanism and application, Nanoscale 13 (2021) 7471–7497, https://doi.org/10.1039/D1NR01113H.
[11] A. vander Straeten, D. Lefèvre, S. Demoustier-Champagne, C. Dupont-Gillain, Protein-based polyelectrolyte multilayers, Adv. Colloïd. Interface Sci. 280 (2020), 102161, https://doi.org/10.1016/j.cis.2020.102161 (1-18).
[12] T. Komatsu, Protein-based microtubes and nanotubes as ultrasmall biomaterials, Chem. Lett. 49 (2020) 1245–1255, https://doi.org/10.1246/cl.200433.
[13] A. Yu, Z. Liang, F. Caruso, Enzyme-multilayer-modified porous membranes as biocatalysts, Chem. Mater. 17 (2005) 171–175, https://doi.org/10.1021/cm048659h?src=recsys.
[14] S. Zhang, S. Demoustier-Champagne, A.M. Jonas, Quantitative collection and enzymatic activity of glucose oxidase nanotubes fabricated by templated layer-by-layer assembly, Biomacromolecules 16 (2015) 2382–2393, https://doi.org/10.1021/acs.biomac.5b00628.
[15] D.G. Ramirez-Wong, C. Bonhomme, S. Demoustier-Champagne, A.M. Jonas, Layer-by-Layer assembly of brushes of vertically-standing enzymatic nanotubes, J. Colloid Interface Sci. 514 (2018) 592–598, https://doi.org/10.1016/j.jcis.2017.12.063.
[16] D.G. Ramirez-Wong, S. Saghazadeh, S. Van Herck, B. De Geest, A.M. Jonas, S. Demoustier-Champagne, Uptake of long protein-polyelectrolyte nanotubes by dendritic cells, Biomacromolecules 18 (2017) 4299–4306, https://doi.org/10.1021/acs.biomac.7b01353.
[17] E. Colaço, D. Lefèvre, E. Maisonhaute, D. Brouri, C. Guibert, C. Dupont-Gillain, K. El Kirat, S. Demoustier-Champagne, J. Landoulsi, Enzyme-assisted mineralization of calcium phosphate: exploring confinement for the design of highly crystalline nano-objects, Nanoscale 12 (2020) 10051–10064, https://doi.org/10.1039/D0NR01638A.
[18] R. Adachi, M. Akiyama, Y. Morita, T. Komatsu, Stratiform protein microtube reactors containing glucose oxidase, Chem. Asian J. 13 (2018) 2796–2799, https://doi.org/10.1002/asia.201800927.
[19] C. Monge, J. Almodovar, T. Boudou, C. Picart, Spatio-temporal control of LbL films for biomedical applications: from 2D to 3D, Adv. Healthc. Mater. 4 (2015) 811–830, https://doi.org/10.1002/adhm.201400715.
[20] S. Park, U. Han, D. Choi, J. Hong, Layer-by-layer assembled polymeric thin films as prospective drug delivery carriers: design and applications, Biomater. Res. 22 (2018) 29, https://doi.org/10.1186/s40824-018-0139-5.
[21] R. Walther, S.M. Nielsen, R. Christiansen, R.L. Meyer, A.N. Zelikin, Combatting implant-associated biofilms through localized drug synthesis, J. Control. Release 287 (2018) 94–102, https://doi.org/10.1016/j.jconrel.2018.08.025.
[22] S. Mariani, V. Robbiano, L.M. Strambini, A. Debrassi, G. Egri, L. Dähne, G. Barillaro, Layer-by-Layer biofunctionalization of nanostructured porous silicon for high sensitivity and high selectivity label-free affinity biosensing, Nat. Commun. 9 (2018) 5256, https://doi.org/10.1038/s41467-018-07723-8.
[23] X. Zhang, L. Huang, Y. Zhang, S. SI, H. Guo, J.Liu Su, Layer-by-layer assembly for immobilizing enzymes in enzymatic biofuel cells, Sustain. Energy Fuels 4 (2020) 68–79, https://doi.org/10.1039/C9SE00643E.
[24] C.H. Kwon, Y. Ko, D. Shin, M. Kwon, J. Park, W.K. Bae, S.W. Lee, J. Cho, High-power hybrid biofuel cells using layer-by-layer assembled glucose oxidase-coated metallic cotton fibers, Nat. Commun. 9 (2018) 4479, https://doi.org/10.1038/s41467-018-06994-5.
[25] C.J. Roy, C. Dupont-Gillain, S. Demoustier-Champagne, A.M. Jonas, J. Landoulsi, Growth mechanism of confined polyelectrolyte multilayers in nanoporous templates, Langmuir 26 (2010) 3350–3355, https://doi.org/10.1021/la903121e.
[26] Y. Cho, C. Lee, J. Hong, Pore size effect on the formation of polymer nanotubular structures within nanoporous templates, Colloids Surf. A: Physicochem. Eng. Asp. 443 (2014) 195–200, https://doi.org/10.1016/j.colsurfa.2013.11.013.

[27] D.G. Ramírez-Wong, C. Coelho-Diogo, C. Aimé, C. Bonhomme, A.M. Jonas, S. Demoustier-Champagne, Effects of geometrical confinement in membrane pores on enzyme-based layer-by-layer assemblies, Appl. Surf. Sci. 338 (2015) 154–162, https://doi.org/10.1016/j.apsusc.2015.02.123.

[28] C. Wang, Z.H. Sheng, J. Ouyang, J.J. Xu, H.Y. Chen, X.H. Xia, Nanoconfinement effects: Glucose oxidase reaction kinetics in nanofluidics, ChemPhysChem 13 (2012) 762–768, https://doi.org/10.1002/cphc.201100842.

[29] C.O. Ania, A. Gomis-Berenguer, J. Dentzer, C. Vix-Guterl, Nanoconfinement of glucose oxidase on mesoporous carbon electrodes with tunable pore sizes, J. Electroanal. Chem. 808 (2018) 372–379, https://doi.org/10.1016/j.jelechem.2017.09.009.

[30] S. Zhang, P. Xin, S. Demoustier-Champagne, A.M. Jonas, Tuning the catalytic activity of enzymes embedded in layer-by-layer assembled films, Colloids Surf. A: Physicochem. Eng. Asp. 631 (2021), 127698, https://doi.org/10.1016/j.colsurfa.2021.127698.

[31] Y. Lvov, K. Ariga, I. Ichinose, T. Kunitake, Molecular film assembly via layer-by-layer adsorption of oppositely charged macromolecules (linear polymer, protein and clay) and concanavalin A and glycogen, Thin Solid Films 284–285 (1996) 797–801, https://doi.org/10.1016/S0040-6090(95)08449-5.

[32] Y. Xie, Z. Li, J. Zhou, Hamiltonian replica exchange simulations of glucose oxidase adsorption on charged surfaces, Phys. Chem. Chem. Phys. 20 (2018) 14587–14596, https://doi.org/10.1039/C8CP00530C.